PROCEEDINGS OF THE ROYAL SOCIETY A

Proc. R. Soc. A (2007) **463**, 2689–2707
doi:10.1098/rspa.2007.1862
Published online 31 July 2007

Asymptotic Green's function in homogeneous anisotropic viscoelastic media

By Václav Vavryčuk*

Geophysical Institute, Boční II/1401, 141 31 Praha 4, Czech Republic

An asymptotic Green's function in homogeneous anisotropic viscoelastic media is derived. The Green's function in viscoelastic media is formally similar to that in elastic media, but its computation is more involved. The stationary slowness vector is, in general, complex valued and inhomogeneous. Its computation involves finding two independent real-valued unit vectors which specify the directions of its real and imaginary parts and can be done either by iterations or by solving a system of coupled polynomial equations. When the stationary slowness direction is found, all quantities standing in the Green's function such as the slowness vector, polarization vector, phase and energy velocities and principal curvatures of the slowness surface can readily be calculated.

The formulae for the exact and asymptotic Green's functions are numerically checked against closed-form solutions for isotropic and simple anisotropic, elastic and viscoelastic models. The calculations confirm that the formulae and developed numerical codes are correct. The computation of the *P*-wave Green's function in two realistic materials with a rather strong anisotropy and absorption indicates that the asymptotic Green's function is accurate at distances greater than several wavelengths from the source. The error in the modulus reaches at most 4% at distances greater than 15 wavelengths from the source.

Keywords: anisotropy; attenuation; Green's function; viscoelasticity

1. Introduction

The theory of waves propagating in viscoelastic media has become increasingly important and intensively developed in recent years (Auld 1973; Caviglia & Morro 1992; Carcione 2001). This concerns studying the basic attributes of homogeneous and inhomogeneous plane waves such as slowness and attenuation vectors (Červený & Pšenčík 2005), deriving formulae for linearized attenuation coefficients (Zhu & Tsvankin 2006, 2007), studying acoustic axes (Shuvalov & Scott 1999; Shuvalov 2001), energy flux (Carcione & Cavallini 1993; Deschamps *et al.* 1997; Boulanger 1998; Červený & Pšenčík 2006) and reflection/transmission coefficients at a plane interface between two homogeneous viscoelastic halfspaces (Borcherdt 1977, 1982; Krebes 1983; Richards 1984; Wennerberg 1985; Nechtschein & Hron 1996; Brokešová 2001; Daley & Krebes 2004). In contrast to plane-wave propagation, considerably less attention has been paid to the theory of waves excited by point or finite sources in isotropic

*vv@ig.cas.cz

Received 7 March 2007
Accepted 4 May 2007

and anisotropic viscoelastic media (Carcione 1994, 2001). So far, such wave fields are usually computed using numerical methods that directly solve the wave equation (Carcione 1990; Saenger & Bohlen 2004; Moczo *et al.* 2007).

In this paper, I will study the waves generated by point sources. I generalize the formula for the exact Green's function in homogeneous anisotropic elastic media (Buchwald 1959; Burridge 1967; Willis 1980; Norris 1994; Wang & Achenbach 1994) to viscoelastic media and present closed-form solutions of the exact viscoelastic Green's function for isotropy and three simple types of anisotropy. Further, I derive the asymptotic Green's function valid for high-frequency signals at distances far from the source and define wave fronts and other asymptotic quantities such as ray velocity and ray attenuation. In numerical modelling, I verify the correctness of the analytical, exact numerical and asymptotic Green's functions, and demonstrate their accuracy and efficiency.

In the following, real and imaginary parts of complex-valued quantities are denoted by superscripts R and I, respectively. A complex-conjugate quantity is denoted by an asterisk. The vector direction of a complex-valued vector $\boldsymbol{v}$ is calculated as $\boldsymbol{v}/\sqrt{\boldsymbol{v}\cdot\boldsymbol{v}}$ (the normalization condition $\boldsymbol{v}/\sqrt{\boldsymbol{v}\cdot\boldsymbol{v}^*}$ is not used because it complicates generalizing some of the real-valued equations to complex-valued ones). If any complex-valued vector is defined by a real-valued direction, it is called homogeneous, and if defined by a complex-valued direction, it is called inhomogeneous. In formulae, the Einstein summation convention is used for repeated subscripts.

2. Anisotropic viscoelastic medium

Let us assume a time-harmonic plane wave described by the displacement vector

$$u_i(\boldsymbol{x},t) = U(\boldsymbol{x})g_i \exp[-\mathrm{i}\omega(t-\boldsymbol{p}\cdot\boldsymbol{x})], \tag{2.1}$$

where $\boldsymbol{x}$ is the position vector; U is the amplitude; $\boldsymbol{g}$ is the unit polarization vector; ω is the circular frequency; and t is the time. Vector $\boldsymbol{p}$ is the slowness vector defined as $\boldsymbol{p}=\boldsymbol{n}/c$, where $\boldsymbol{n}$ is the slowness direction and c is the phase velocity. The plane wave propagates in the viscoelastic medium defined by the following stress–strain relation:

$$\sigma_{ij} = c^{\mathrm{R}}_{ijkl}e_{kl} + \eta_{ijkl}\dot{e}_{kl}, \tag{2.2}$$

where σ_{ij} are the components of the stress tensor; e_{kl} are the components of the strain tensor; $\dot{e}_{kl}$ is the time derivative of e_{kl}; and c^{R}_{ijkl} and η_{ijkl} are the components of the elasticity and viscosity tensors, respectively. These tensors must be positive definite to ensure that strain energy W and dissipation energy rate R are positive,

$$W = \tfrac{1}{2}\, c^{\mathrm{R}}_{ijkl}e_{ij}e_{kl} > 0 \qquad \text{and} \qquad R = \tfrac{1}{2}\eta_{ijkl}\dot{e}_{ij}\dot{e}_{kl} > 0. \tag{2.3}$$

Taking into account that $\dot{e}_{kl}$ is expressed for the time-harmonic wave (2.1) as

$$\dot{e}_{kl} = -\mathrm{i}\omega e_{kl}, \tag{2.4}$$

the stress–strain relation (2.2) can be formally written in the frequency domain in a form identical with that for elastic media, where the real-valued elasticity tensor c^{R}_{ijkl} is substituted by the complex-valued frequency-dependent viscoelasticity tensor c_{ijkl},

$$c_{ijkl} = c^{\mathrm{R}}_{ijkl} - \mathrm{i}\omega\eta_{ijkl}. \tag{2.5}$$

This tensor is used to construct the complex-valued density-normalized viscoelasticity tensor $a_{ijkl} = c_{ijkl}/\rho$, and subsequently the complex-valued Christoffel tensor Γ_{jk}, defined alternatively in terms of slowness direction $\boldsymbol{n}$,

$$\Gamma_{jk}(\boldsymbol{n}) = a_{ijkl} n_i n_l, \tag{2.6}$$

or slowness vector $\boldsymbol{p}$,

$$\Gamma_{jk}(\boldsymbol{p}) = a_{ijkl} p_i p_l. \tag{2.7}$$

Slowness direction $\boldsymbol{n}$ is real valued for homogeneous waves, but complex valued for inhomogeneous waves.

The Christoffel tensor Γ_{jk} has three eigenvalues and three eigenvectors, which define the properties of three plane waves propagating in anisotropic media. Eigenvalues $G(\boldsymbol{n})$ and $G(\boldsymbol{p})$ read

$$G(\boldsymbol{n}) = a_{ijkl} n_i n_l g_j g_k = c^2 \quad \text{and} \tag{2.8}$$

$$G(\boldsymbol{p}) = a_{ijkl} p_i p_l g_j g_k = 1 \tag{2.9}$$

and define phase velocity c and slowness vector $\boldsymbol{p}$ as a function of slowness direction $\boldsymbol{n}$. The eigenvectors define polarization vectors $\boldsymbol{g}$. The polarization vectors are normalized so that $\boldsymbol{g}\cdot\boldsymbol{g}=1$. Note that when applying condition $\boldsymbol{g}\cdot\boldsymbol{g}^*=1$, equations (2.8) and (2.9) would have a different form also containing complex-conjugate quantities.

Using the eigenvalue $G(\boldsymbol{p})$, we define the energy velocity vector as

$$v_i = \frac{1}{2}\frac{\partial G}{\partial p_i} = a_{ijkl} p_l g_j g_k, \tag{2.10}$$

which is called the group velocity vector in elastic media. Vectors $\boldsymbol{v}$ and $\boldsymbol{p}$ are related by the equation $\boldsymbol{v}\cdot\boldsymbol{p}=1$. The slowness vector, phase velocity, energy velocity and the polarization vectors are in general complex valued.

3. Exact Green's function

(*a*) *Elastic medium*

The exact elastodynamic Green's function in unbounded, homogeneous, anisotropic, perfectly elastic media can be expressed in the frequency domain as the sum of regular and singular terms, $G^{\mathrm{r}}_{kl}(\boldsymbol{x},\omega)$ and $G^{\mathrm{s}}_{kl}(\boldsymbol{x},\omega)$, as follows

(Norris 1994, eqn. (3.22); Wang & Achenbach 1994, eqns (17)–(21)):

$$G_{kl}^{\mathrm{exact}}(\boldsymbol{x},\omega) = G_{kl}^{\mathrm{r}}(\boldsymbol{x},\omega) + G_{kl}^{\mathrm{s}}(\boldsymbol{x}), \tag{3.1}$$

$$G_{kl}^{\mathrm{r}}(\boldsymbol{x},\omega) = \frac{\mathrm{i}\omega}{8\pi^2\rho}\sum_{M=1}^{3}\int\limits_{\substack{S(\boldsymbol{n})\\ \boldsymbol{n}\cdot\boldsymbol{x}>0}} \frac{g_k^{(M)} g_l^{(M)}}{\left(c^{(M)}\right)^3}\exp\left(\mathrm{i}\omega\frac{\boldsymbol{n}\cdot\boldsymbol{x}}{c^{(M)}}\right)\mathrm{d}S(\boldsymbol{n}) \quad \text{and} \tag{3.2}$$

$$G_{kl}^{\mathrm{s}}(\boldsymbol{x}) = \frac{1}{8\pi^2\rho}\sum_{M=1}^{3}\int\limits_{S(\boldsymbol{n})} \frac{g_k^{(M)} g_l^{(M)}}{\left(c^{(M)}\right)^2}\,\delta(\boldsymbol{n}\cdot\boldsymbol{x})\;\mathrm{d}S(\boldsymbol{n}), \tag{3.3}$$

where the superscript $M=1$, 2 and 3 denotes the type of wave (P, $S1$ and $S2$); $\boldsymbol{g}=\boldsymbol{g}(\boldsymbol{n})$ is the unit polarization vector; $c=c(\boldsymbol{n})$ is the phase velocity; ρ is the density of the medium; ω is the circular frequency; $\boldsymbol{x}=\boldsymbol{N}r$ is the position vector; r is the distance of the observation point from the source; $\boldsymbol{N}$ is the ray vector; $\boldsymbol{n}$ is the slowness direction; and $S(\boldsymbol{n})$ is the unit sphere. The regular term is integrated over a hemisphere, defined by $\boldsymbol{n}\cdot\boldsymbol{x}>0$. The singular term is integrated over a unit circle defined by $\boldsymbol{n}\cdot\boldsymbol{x}=0$. The reduction of the surface integral to a line integral in the singular term is due to the Dirac delta function $\delta(\boldsymbol{n}\cdot\boldsymbol{x})$ in the integrand. Since the singular term does not depend on frequency ω, it physically corresponds to the static Green's function.

All quantities in (3.1)–(3.3) are real valued, including slowness direction $\boldsymbol{n}$. Hence, the regular part of the exact Green's function is calculated as a superposition of homogeneous plane waves. This is the essential advantage of formulae (3.1)–(3.3) compared with other formulae for the Green's function which also involve inhomogeneous waves specified by a complex-valued slowness direction $\boldsymbol{n}$ (e.g. the Green's function in isotropic media calculated using the Weyl integral; see Aki & Richards 2002, §6.1).

Formulae (3.1)–(3.3) can be derived in several alternative ways. Probably, the most straightforward way is to solve the elastodynamic equation in the slowness-frequency domain to obtain $G_{kl}(\boldsymbol{p},\omega)$. Subsequently, $G_{kl}(\boldsymbol{x},\omega)$ is calculated by applying the inverse three-dimensional Fourier transform (see Mura 1987; Norris 1994; Červený 2001), which physically corresponds to a superposition of homogeneous plane waves propagating in an arbitrary direction with an arbitrary phase velocity. Using the residuum theorem, the volume integral is further reduced to a surface integral representing a superposition of homogeneous plane waves propagating in an arbitrary direction, but with the phase velocity satisfying equation (2.8).

The integration in (3.2) and (3.3) can also be performed over slowness surface $S(\boldsymbol{p})$. Taking into account the relation between surface elements $\mathrm{d}S(\boldsymbol{n})$ and $\mathrm{d}S(\boldsymbol{p})$ (see Burridge 1967),

$$\boldsymbol{n}\cdot\boldsymbol{N}\;\mathrm{d}S(\boldsymbol{p}) = p^2\;\mathrm{d}S(\boldsymbol{n}) \tag{3.4}$$

and the relation between the phase and energy velocities c and v,

$$\boldsymbol{n}\cdot\boldsymbol{N} = \frac{c}{v}, \tag{3.5}$$

we can put for a particular wave (P, $S1$ or $S2$)

$$G^{\mathrm{r}}_{kl}(\boldsymbol{x},\omega) = \frac{\mathrm{i}\omega}{8\pi^2\rho} \int\limits_{\substack{S(\boldsymbol{p}) \\ \boldsymbol{n}\cdot\boldsymbol{x}>0}} \frac{g_k g_l}{v} \exp(\mathrm{i}\omega \boldsymbol{p}\cdot\boldsymbol{x})\, \mathrm{d}S(\boldsymbol{p}) \quad \text{and} \tag{3.6}$$

$$G^{\mathrm{s}}_{kl}(\boldsymbol{x}) = \frac{1}{8\pi^2\rho} \int\limits_{S(\boldsymbol{p})} \frac{g_k g_l}{v} \delta(\boldsymbol{p}\cdot\boldsymbol{x})\, \mathrm{d}S(\boldsymbol{p}). \tag{3.7}$$

The complete Green's function is then a sum of contributions of all three waves.

(*b*) *Viscoelastic medium*

The Green's function in viscoelastic media is derived in a quite analogous way as in elastic media. The Green's function is calculated by applying the inverse three-dimensional Fourier transform, which physically corresponds to a superposition of homogeneous plane waves propagating in an arbitrary direction with an arbitrary (real-valued) phase velocity. Using the residuum theorem, the volume integral is reduced to a surface integral representing a superposition of homogeneous plane waves propagating in an arbitrary direction, but with complex-valued velocities satisfying equation (2.8) and with polarization vectors satisfying the Christoffel equation. Hence, the Green's function is expressed by exactly the same formulae as formulae (3.1)–(3.3), (3.6) and (3.7) derived for elastic media. The only difference is that some quantities in the integrands become complex valued and frequency dependent. This concerns phase velocity c, slowness vector $\boldsymbol{p}$, energy velocity v and polarization vector $\boldsymbol{g}$. Slowness direction $\boldsymbol{n}$, ray direction $\boldsymbol{N}$, position vector $\boldsymbol{x}$ and density ρ remain real valued and do not depend on real-valued frequency ω. Since some quantities in (3.3) and (3.7) are frequency dependent, the singular term of the Green's function becomes also frequency dependent $G^{\mathrm{s}}_{kl} = G^{\mathrm{s}}_{kl}(\boldsymbol{x},\omega)$.

Emphasize that $\boldsymbol{p}$ is a homogeneous complex-valued vector; hence its direction $\boldsymbol{n}$ in (3.1)–(3.3) remains real valued. This is in agreement with the above statement that the exact Green's function in viscoelastic media is calculated as a superposition of homogeneous plane waves, similarly as in elastic media.

4. Asymptotic Green's function

Since the exact Green's function is expressed in terms of complicated integrals, it is advantageous to evaluate the Green's function asymptotically. Physically, it corresponds to studying the high-frequency Green's function in the far field, i.e. at distances far from the source with respect to the predominant wavelength of the wave field. The asymptotic Green's function significantly simplifies, because the singular term (3.7) is negligible for high frequencies, and the regular term (3.6) can be calculated using the stationary phase method for the elastic medium or the steepest descent method for the viscoelastic medium.

(a) Elastic medium

Formula (3.6) can be expressed as

$$G_{kl}^{\mathrm{r}}(\boldsymbol{x},\omega)=\frac{\mathrm{i}\omega}{8\pi^2\rho}\int\limits_{\substack{S(\boldsymbol{p})\\ \theta(\boldsymbol{p})>0}} P_{kl}(\boldsymbol{p})\exp(\mathrm{i}\lambda\theta(\boldsymbol{p}))\,\mathrm{d}S(\boldsymbol{p}), \tag{4.1}$$

where

$$P_{kl}(\boldsymbol{p})=\frac{g_k(\boldsymbol{p})g_l(\boldsymbol{p})}{v(\boldsymbol{p})} \quad \text{and} \quad \theta(\boldsymbol{p})=\boldsymbol{p}\cdot\boldsymbol{N}. \tag{4.2}$$

Functions $P_{kl}(\boldsymbol{p})$ and $\theta(\boldsymbol{p})$ are assumed to be smooth, and the parameter $\lambda=\omega r$ is large and positive. Phase $\theta(\boldsymbol{p})$ is positive inside the integration area and zero at its boundary. Expanding phase function $\theta(\boldsymbol{p})$ near stationary point $\boldsymbol{p}_0$, defined by

$$\frac{\partial\theta(\boldsymbol{p})}{\partial s_1}\Big|_{\boldsymbol{p}=\boldsymbol{p}_0}=0, \qquad \frac{\partial\theta(\boldsymbol{p})}{\partial s_2}\Big|_{\boldsymbol{p}=\boldsymbol{p}_0}=0, \tag{4.3}$$

yields

$$\theta(\boldsymbol{p})=\boldsymbol{p}_0\cdot\boldsymbol{N}-\tfrac{1}{2}\big(K_1s_1^2+K_2s_2^2\big), \tag{4.4}$$

where K_1 and K_2 are the principal curvatures of the slowness surface at $\boldsymbol{p}_0$, and s_1 and s_2 are the local coordinates defined on the slowness surface. The coordinate axes have their origin at $\boldsymbol{p}_0$ and point along the principal curvatures of the slowness surface at $\boldsymbol{p}_0$. The third coordinate axis s_3 is normal to the slowness surface at $\boldsymbol{p}_0$ and parallel to $\boldsymbol{N}$.

Applying the stationary phase method to integral (4.1), we obtain the asymptotic Green's function $G_{kl}^{\mathrm{asym}}(\boldsymbol{x},\omega)$ in the following form (Buchwald 1959; Burridge 1967; Every & Kim 1994; Červený 2001, eqn. (2.5.75)):

$$G_{kl}^{\mathrm{asym}}(\boldsymbol{x},\omega)=\frac{1}{4\pi\rho}\,\frac{g_kg_l}{v\sqrt{|K|}}\,\frac{1}{r}\exp\Big(\mathrm{i}\frac{\pi}{2}\sigma_0+\mathrm{i}\omega\boldsymbol{p}_0\cdot\boldsymbol{x}\Big), \tag{4.5}$$

where $K=K_1K_2$ is the Gaussian curvature of the slowness surface, and σ_0 is defined as

$$\sigma_0=1-\tfrac{1}{2}\operatorname{sgn}K_1-\tfrac{1}{2}\operatorname{sgn}K_2. \tag{4.6}$$

Both the principal curvatures K_1 and K_2 are positive for a convex surface, negative for a concave surface, and of opposite signs for a saddle-shaped surface. All quantities dependent on $\boldsymbol{p}$ in (4.5) are taken at stationary point $\boldsymbol{p}_0$. Formula (4.5) works for all directions except for singularities on the slowness surface and cusp edges on the wave front, where a more involved approach is required (Vavryčuk 1999, 2002; Gridin 2000).

(b) Viscoelastic medium

Since phase velocity c is complex valued in viscoelastic media, the slowness vector $\boldsymbol{p}$ and functions $P_{kl}(\boldsymbol{p})$ and $\theta(\boldsymbol{p})$ in (4.1) are also complex valued. Parameter λ is real, large and positive. The integration in (4.1) is over complex-valued slowness

surface $S(\boldsymbol{p})$. The stationary point $\boldsymbol{p}_0$ on $S(\boldsymbol{p})$ is defined by

$$\frac{\partial\theta(\boldsymbol{p})}{\partial s_1}\Big|_{\boldsymbol{p}=\boldsymbol{p}_0}=0, \qquad \frac{\partial\theta(\boldsymbol{p})}{\partial s_2}\Big|_{\boldsymbol{p}=\boldsymbol{p}_0}=0, \tag{4.7}$$

where s_1 and s_2 are the complex-valued local coordinates defined on $S(\boldsymbol{p})$. The third complex-valued coordinate axis s_3 is normal to the slowness surface at $\boldsymbol{p}_0$ and parallel to $\boldsymbol{N}$. Since $\boldsymbol{N}$ is a real-valued vector, the s_3-axis is homogeneous. Consequently, the energy velocity vector,

$$\boldsymbol{v}=v\boldsymbol{N}=\frac{1}{2}\frac{\partial G}{\partial \boldsymbol{p}}\Big|_{\boldsymbol{p}=\boldsymbol{p}_0} \tag{4.8}$$

must also be homogeneous. Expanding phase function $\theta(\boldsymbol{p})$ near stationary point $\boldsymbol{p}_0$ yields

$$\theta(\boldsymbol{p})=\boldsymbol{p}_0\cdot\boldsymbol{N}-\tfrac{1}{2}\big(K_1 s_1^2+K_2 s_2^2\big), \tag{4.9}$$

where K_1 and K_2 are the complex-valued principal curvatures of the slowness surface at $\boldsymbol{p}_0$. Applying the steepest descent method (Ben-Menahem & Singh 1981, appendix E) to integral (4.1), we obtain

$$G_{kl}^{\mathrm{asym}}(\boldsymbol{x},\omega)=\frac{\mathrm{i}\omega}{8\pi^2\rho}P_{kl}(\boldsymbol{p}_0)\sqrt{\frac{2\pi}{\mathrm{i}\lambda K_1}}\sqrt{\frac{2\pi}{\mathrm{i}\lambda K_2}}\exp(\mathrm{i}\lambda\theta(\boldsymbol{p}_0)) \tag{4.10}$$

and finally

$$G_{kl}^{\mathrm{asym}}(\boldsymbol{x},\omega)=\frac{1}{4\pi\rho}\,\frac{g_k g_l}{v\sqrt{|K|}}\,\frac{1}{r}\exp(\mathrm{i}\sigma_0+\mathrm{i}\omega\boldsymbol{p}_0\cdot\boldsymbol{x}), \tag{4.11}$$

where

$$\sigma_0=-\frac{1}{2}(\varphi_1+\varphi_2), \quad -\frac{3}{2}\pi\le\varphi_1<\frac{1}{2}\pi, \quad -\frac{3}{2}\pi\le\varphi_2<\frac{1}{2}\pi.$$

Angles φ_1 and φ_2 define the phases of the principal curvatures K_1 and K_2, and $|K|$ is the modulus of the Gaussian curvature $K=K_1K_2$. All quantities dependent on $\boldsymbol{p}$ in (4.11) are taken at stationary point $\boldsymbol{p}_0$. Position vector $\boldsymbol{x}$, distance r, frequency ω, phase angles φ_1 and φ_2 and density ρ are real valued, but polarization vector $\boldsymbol{g}$, Gaussian curvature K, principal curvatures K_1 and K_2, energy velocity v and slowness vector $\boldsymbol{p}_0$ are complex valued. Similarly as for elastic media, formula (4.11) fails in singularities.

Decomposing the energy velocity v into real and imaginary parts, v^{R} and v^{I}, the exponential term in (4.11) becomes

$$\exp(\mathrm{i}\omega\boldsymbol{p}_0\cdot\boldsymbol{x})=\exp\Big(\mathrm{i}\omega\frac{r}{v}\Big)=\exp(-\omega A^{\mathrm{ray}}r)\exp\Big(\mathrm{i}\omega\frac{r}{V^{\mathrm{ray}}}\Big), \tag{4.12}$$

where

$$V^{\mathrm{ray}} = \frac{vv^*}{v^{\mathrm{R}}} = \frac{v^{\mathrm{R}}v^{\mathrm{R}} + v^{\mathrm{I}}v^{\mathrm{I}}}{v^{\mathrm{R}}} \quad \text{and} \tag{4.13}$$

$$A^{\mathrm{ray}} = -\frac{v^{\mathrm{I}}}{vv^*} = -\frac{v^{\mathrm{I}}}{v^{\mathrm{R}}v^{\mathrm{R}} + v^{\mathrm{I}}v^{\mathrm{I}}}. \tag{4.14}$$

The asterisk in (4.13) and (4.14) indicates a complex-conjugate quantity. Consequently, the Green's function reads

$$G_{kl}^{\mathrm{asym}}(\boldsymbol{x},\omega) = \frac{1}{4\pi\rho}\,\frac{g_k g_l}{v\sqrt{|K|}}\,\frac{\exp(-\omega A^{\mathrm{ray}} r)}{r}\exp\Big(\mathrm{i}\sigma_0 + \mathrm{i}\omega\frac{r}{V^{\mathrm{ray}}}\Big). \tag{4.15}$$

Since V^{ray} and A^{ray} control the propagation velocity and attenuation along a ray, I will refer to them as the ray velocity and ray attenuation, respectively.

5. Numerical procedure

(*a*) *Stationary point*

Determining stationary point $\boldsymbol{p}_0$ is the crucial and the most complicated step in calculating the asymptotic quantities in anisotropic viscoelastic media. Although the exact Green's function (3.1)–(3.3) is calculated as a superposition of homogeneous plane waves, the asymptotic Green's function is calculated at a stationary point which corresponds to an inhomogeneous plane wave. Hence, the slowness direction at the stationary point is no longer real valued, but it is generally complex valued.

The complex-valued stationary point $\boldsymbol{p}_0$ can be determined either by iterations or by solving a system of polynomial equations. The iterative procedure is fast and works well provided the wave front is free of triplications. The procedure is based on seeking a complex-valued slowness direction $\boldsymbol{n}_0$, for which energy velocity $\boldsymbol{v}$ is homogeneous and points along a specified ray vector $\boldsymbol{N}$. This represents an inversion for four unknown angles: two angles define the real part and two others define the imaginary part of $\boldsymbol{n}_0$. We can consider the modulus of the complex-valued deviation between the given and predicted ray vectors as the misfit function. The inversion is nonlinear and can be performed using standard methods (Press *et al.* 2002). If the wave front displays triplications, determination of stationary slowness $\boldsymbol{p}_0$ is more involved. When using iterations, we have to be careful to find all slowness vectors corresponding to a given ray, which may sometimes be tricky. The other possibility is to follow Vavryčuk (2006*a*) and solve a system of polynomial equations for the unknown components of $\boldsymbol{p}_0$.

(*b*) *Principal curvatures of the slowness surface*

The principal curvatures of the slowness surface K_1 and K_2 can conveniently be calculated using the wave metric tensor H (Vavryčuk 2003, eqn. (9)),

$$H_{ij} = \frac{1}{2}\,\frac{\partial^2 G}{\partial p_i \partial p_j} = \frac{\partial v_i}{\partial p_j}, \tag{5.1}$$

which is expressed for the P wave as follows (Vavryčuk 2003, eqn. (17)):

$$H_{il}^{(1)} = a_{ijkl} g_j^{(1)} g_k^{(1)} + \frac{v_i^{(12)} v_l^{(12)}}{G^{(1)} - G^{(2)}} + \frac{v_i^{(13)} v_l^{(13)}}{G^{(1)} - G^{(3)}}, \tag{5.2}$$

$$v_i^{(MN)} = a_{ijkl} p_l \left(g_j^{(M)} g_k^{(N)} + g_j^{(N)} g_k^{(M)} \right) \quad \text{and} \tag{5.3}$$

$$G^{(M)} = a_{ijkl} p_i p_l g_j^{(M)} g_k^{(M)}, \tag{5.4}$$

where superscripts M and N denote the type of wave (P, $S1$ or $S2$). The wave metric tensors of the $S1$ or $S2$ waves are analogous (see Vavryčuk 2003, eqns (18) and (19)). The diagonal form of H reads (Klimeš 2002)

$$\mathsf{H}^{\mathrm{diag}} = v \begin{bmatrix} K_1 & & \\ & K_2 & \\ & & v \end{bmatrix}, \tag{5.5}$$

hence principal curvatures K_1 and K_2 can directly be calculated from the eigenvalues of H. Subsequently, Gaussian curvature K is calculated as (Klimeš 2002, eqn. (45))

$$K = \frac{1}{v^4} \det(H_{il}). \tag{5.6}$$

The formulae for the principal and Gaussian curvatures work safely in all directions except for singularities, in which $G^{(1)} = G^{(2)}$ or $G^{(1)} = G^{(3)}$. In such directions and in their close vicinity, equation (5.2) fails.

6. Examples

In this section, the derived formulae are validated on numerical examples. First, the formulae are checked against simple closed-form solutions. Second, the formulae are applied to exemplify the properties of the Green's function in realistic anisotropic viscoelastic materials.

(*a*) *Test models*

For isotropic and some simple anisotropic media, the Green's function can be expressed in closed form. The existing closed-form solutions have been derived for elastic media, but they can simply be generalized to be applicable also to viscoelastic media (see appendices A and B). Subsequently, the viscoelastic closed-form Green's functions can be used to verify the derived formulae and to test numerical codes.

I adopted two viscoelastic and two elastic test models. The first viscoelastic model is isotropic with parameters in the Voigt notation: $a_{11} = 30 - 1.5i$, $a_{44} = 10 - 0.5i$, and with density $\rho = 1$; and the second viscoelastic model is transversely isotropic with parameters: $a_{11} = a_{22} = a_{33} = 25 - 2.5i$, $a_{44} = a_{55} = 10 - i$, $a_{66} = 4 - 0.4i$, $a_{12} = a_{11} - 2a_{66}$, $a_{13} = a_{23} = a_{11} - 2a_{44}$, and with

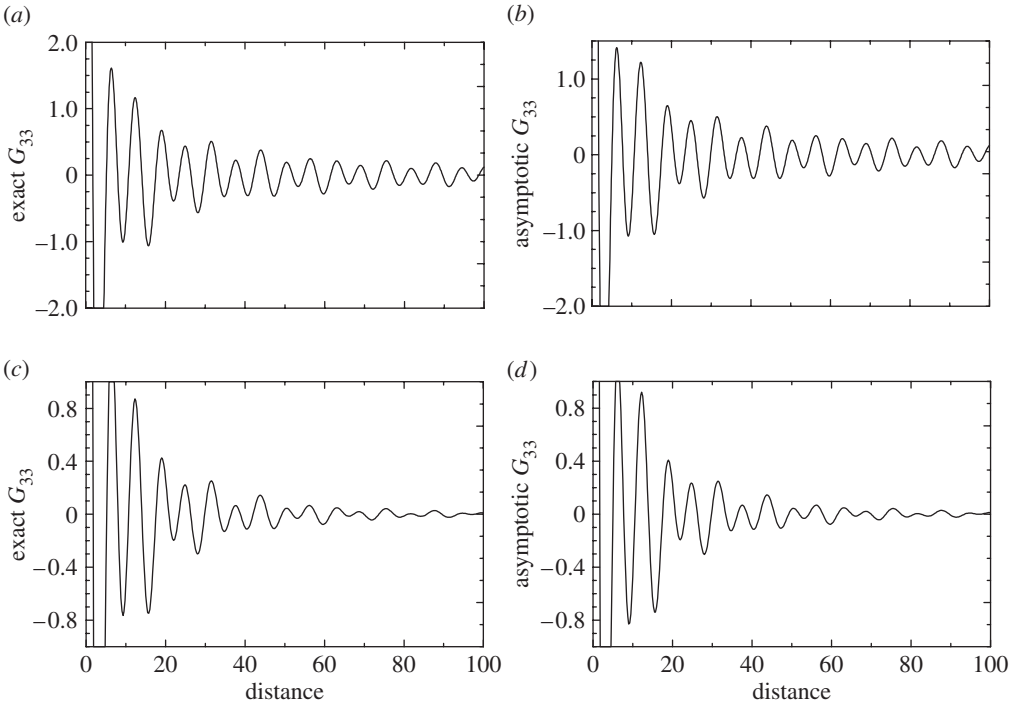

Figure 1. The real part of the G_{33} component of the Green's function for isotropic (a,b) elastic and (c,d) viscoelastic media. The exact Green's function in (a,c) is calculated using equations (3.1)–(3.3) and compared with the closed-form solution (A 1). The asymptotic Green's function in (b,d) is calculated using (4.11) and compared with the far-field term of solution (A 1). The distance is normalized to $\sqrt{a_{44}^{\mathrm{R}}}/\omega$. The Green's functions are calculated for a ray deviating by angle $\theta = 45°$ from the vertical.

density $\rho = 1$. The elastic models are described by real parts of the above viscoelastic parameters. The circular frequency ω of the wave field equals 1.

For the four models, I calculated the exact Green's function by direct numerical calculation of integrals (3.2) and (3.3), an asymptotic Green's function (4.11) and the exact and far-field analytical Green's functions using (A 1) and (B 3). Figures 1 and 2 show the Green's functions in both the elastic and viscoelastic models. The exact solution obtained using the numerical integration coincides with the analytical solution within the width of the line. Similarly, the asymptotic solution perfectly coincides with the analytic far-field approximation. This validates the formulae derived as well as the codes developed.

(*b*) *Real models*

The Green's function is calculated in two anisotropic viscoelastic materials: clay shale and carbon-epoxy composite (see table 1). The materials display anisotropy in velocities as well as in attenuation. The values for the clay shale were taken from Carcione & Cavallini (1995) and those for the carbon-epoxy composite from Hosten *et al.* (1987). The values were slightly modified to make the models transversely isotropic (see table 2).

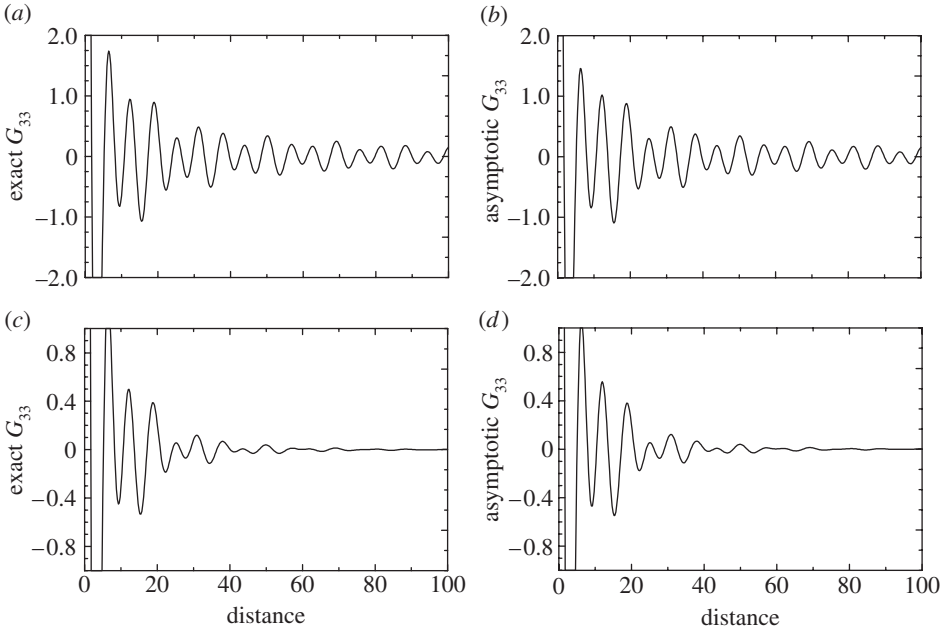

Figure 2. The real part of the G_{33} component of the Green's function for transversely isotropic (a,b) elastic and (c,d) viscoelastic media. The exact Green's function in (a,c) is calculated using equations (3.1)–(3.3) and compared with the closed-form solution (B 3). The asymptotic Green's function in (b,d) is calculated using (4.11) and compared with the far-field term of solution (B 3). The distance is normalized to $\sqrt{a^{\mathrm{R}}_{44}/\omega}$. The Green's functions are calculated for a ray deviating by angle $\theta = 45°$ from the vertical.

Figure 3 shows the basic properties of the P waves propagating in the materials studied: the left-hand plots show the directional dependence of ray velocity V^{ray} and real-valued phase velocity V^{phase}, and the right-hand plots show the directional dependence of ray attenuation A^{ray} and of phase attenuation A^{phase}. The ray velocity and ray attenuation characterize the propagation velocity and attenuation along a ray, while the phase velocity and phase attenuation characterize the propagation velocity and attenuation along the normal to the plane wave front. The magnitudes of the phase quantities are calculated from the complex-valued slowness vector $\boldsymbol{p}$ as

$$V^{\mathrm{phase}} = \frac{1}{\sqrt{\boldsymbol{p}^{\mathrm{R}}\cdot\boldsymbol{p}^{\mathrm{R}}}}, \qquad A^{\mathrm{phase}} = \frac{\boldsymbol{p}^{\mathrm{I}}\cdot\boldsymbol{p}^{\mathrm{R}}}{\sqrt{\boldsymbol{p}^{\mathrm{R}}\cdot\boldsymbol{p}^{\mathrm{R}}}} \tag{6.1}$$

and their direction is along the normal to the plane wave front,

$$\boldsymbol{n}^{\mathrm{phase}} = \frac{\boldsymbol{p}^{\mathrm{R}}}{\sqrt{\boldsymbol{p}^{\mathrm{R}}\cdot\boldsymbol{p}^{\mathrm{R}}}}. \tag{6.2}$$

The magnitudes of the ray quantities are defined by (4.13) and (4.14) and they point along ray vector $\boldsymbol{N}$. Emphasize that slowness vector $\boldsymbol{p}$ is stationary for both the ray and phase quantities; hence it is, in general, an inhomogeneous complex-valued vector. The corresponding energy velocity vector $\boldsymbol{v}$ must be homogeneous, and ray vector $\boldsymbol{N} = \boldsymbol{v}/v$ is real valued.

Table 1. Viscoelastic parameters. (Matrix of quality factors $\boldsymbol{Q}$ is defined as $Q_{KL}=-c^{\mathrm{R}}_{KL}/c^{\mathrm{I}}_{KL}$, K, $L=1, \ldots, 6$. The two-index Voigt notation is used for viscoelastic parameters. The clay shale model is taken from Carcione & Cavallini (1995) and the carbon-epoxy model is from Hosten *et al.* (1987).)

model	c^{R}_{11} (GPa)	c^{R}_{13} (GPa)	c^{R}_{33} (GPa)	c^{R}_{44} (GPa)	c^{R}_{66} (GPa)	ρ (kg m^{-3})
clay shale	68.7	40.1	42.0	11.4	24.2	2590
carbon-epoxy	15.0	3.4	87.0	7.8	3.9	1595
model	Q_{11}	Q_{13}	Q_{33}	Q_{44}	Q_{66}	f (Hz)
clay shale	29.7	52.8	18.2	20.3	31.1	20
carbon-epoxy	34.1	2.4	5.4	59.1	36.5	5×10^{6}

Table 2. P-wave anisotropy of velocity and attenuation. ($\bar{V}^{\mathrm{ray}}$ is the mean P-wave ray velocity, $a^{\mathrm{ray}}_{\mathrm{V}}$ the P-wave velocity anisotropy, $\bar{A}^{\mathrm{ray}}$ the mean P-wave ray attenuation and $a^{\mathrm{ray}}_{\mathrm{Q}}$ the P-wave ray attenuation anisotropy. The velocity and attenuation anisotropy is calculated as $a^{\mathrm{ray}}_{\mathrm{V}}=200\big(V^{\mathrm{ray}}_{\mathrm{MAX}}-V^{\mathrm{ray}}_{\mathrm{MIN}}\big)/\big(V^{\mathrm{ray}}_{\mathrm{MAX}}+V^{\mathrm{ray}}_{\mathrm{MIN}}\big)$ and $a^{\mathrm{ray}}_{\mathrm{Q}}=200\big(A^{\mathrm{ray}}_{\mathrm{MAX}}-A^{\mathrm{ray}}_{\mathrm{MIN}}\big)/\big(A^{\mathrm{ray}}_{\mathrm{MAX}}+A^{\mathrm{ray}}_{\mathrm{MIN}}\big)$, where subscripts MAX and MIN indicate the maximum and minimum values over all rays.)

model	$\bar{V}^{\mathrm{ray}}$ (10^{3} m s^{-1})	$a^{\mathrm{ray}}_{\mathrm{V}}$ (%)	$\bar{A}^{\mathrm{ray}}$ (10^{-7} s m^{-1})	$a^{\mathrm{ray}}_{\mathrm{Q}}$ (%)
clay shale	4.63	24.4	46.7	71.0
carbon-epoxy	4.35	83.7	81.1	88.0

Figure 4 shows a comparison of the exact and asymptotic P-wave Green's functions for the two materials studied. The figure indicates that the asymptotic Green's function approximates the exact Green's function quite efficiently. As expected, the fit improves with increasing distance from the source. At distance of 15 wavelengths from the source, the error in the modulus of the asymptotic Green's function is approximately 4% or less for all four examples in figure 4.

7. Conclusion

The exact Green's function in homogeneous anisotropic viscoelastic media is calculated as in elastic media by numerically integrating surface and line integrals. The surface integral defines the regular part of the Green's function and physically corresponds to a superposition of homogeneous plane waves. The line integral defines the singular part of the Green's function. While all quantities in the integrals are real valued in elastic media, some of them become complex valued and frequency dependent in viscoelastic media. However, this difference is minor and does not pose complications to computing the Green's function. The complex-valued integrals can be calculated either directly using numerical integration or asymptotically using the steepest descent method. In some very simple cases, the integrals can also be calculated analytically yielding closed-form solutions.

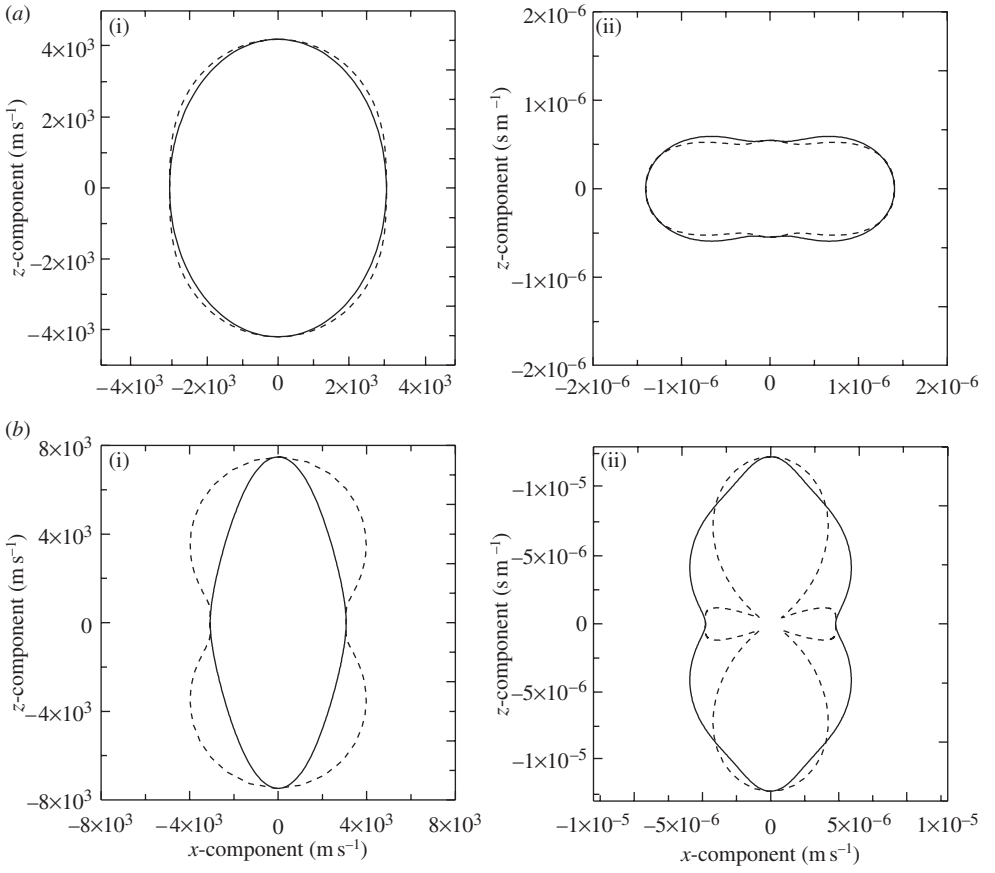

Figure 3. The *P*-wave velocity and attenuation in (*a*) clay shale and (*b*) carbon-epoxy composite. (*a*(i)) Velocities in clay shale, (*a*(ii)) attenuation in clay shale, (*b*(i)) velocities in carboxy-expoxy composite, (*b*(ii)) attenuation in carboxy-epoxy composite. Solid line, ray quantities; dashed line, phase quantities.

The calculation of the asymptotic Green's function is more involved in viscoelastic media than in elastic media. Although the exact Green's function in viscoelastic media is calculated as a superposition of homogeneous plane waves, the asymptotic Green's function is calculated at a stationary point which corresponds to an inhomogeneous plane wave. In elastic media, we usually start with setting a slowness vector and then calculate the corresponding ray direction. The slowness vector is always homogeneous. In viscoelastic media, we first define the ray direction and seek the slowness vector that predicts the vector of the energy velocity parallel to the ray. Since the ray direction is real, the energy velocity vector is homogeneous. Consequently, the stationary slowness vector is, in general, inhomogeneous and its computation involves finding two independent unit vectors, which specify the directions of its real and imaginary parts. This can be done iteratively in a simple way, provided the wave surface is free of triplications. If not, we have to take care of getting all slowness vectors corresponding to a given ray, or we have to solve a system of polynomial equations.

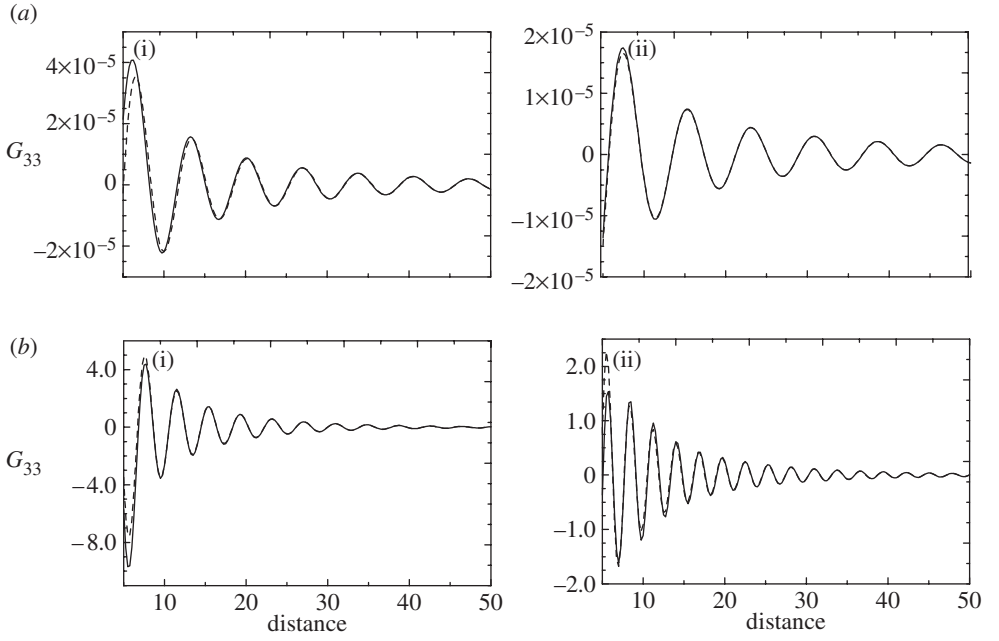

Figure 4. The real part of the G_{33} component of the exact and asymptotic P-wave Green's function in (a) clay shale and (b) carbon-epoxy composite. Solid line, the exact Green's function calculated using equations (3.1)–(3.3); dashed line, the asymptotic Green's function calculated using equation (4.11). The Green's functions are for a ray deviating from the vertical by angle (i) $\theta = 30°$ and (ii) $\theta = 60°$. The distance is normalized to $\sqrt{a^{\mathrm{R}}_{33}}/\omega$. The Green's function is in $10^{-10}\,\mathrm{m\,s^{-1}}$.

I thank Colin Thomson for discussions on the subject, and Klaus Helbig and two anonymous referees for their comments. This work was supported by the grant Agency of the Czech Republic, grant no. 205/05/2182 and by the Consortium Project SW3D 'Seismic Waves in Complex 3-D Structures'.

Appendix A. Green's function in an isotropic viscoelastic medium

Solving integrals (3.2) and (3.3) for a homogeneous isotropic viscoelastic medium, we arrive at the exact viscoelastic Green's function in a form quite analogous to that for an elastic medium (Aki & Richards 2002, eqn. (4.35)). Hence,

$$
\begin{aligned}
G_{kl}^{\mathrm{exact}}(\boldsymbol{x},\omega) &= G_{kl}^{\mathrm{near}}(\boldsymbol{x},\omega) + G_{kl}^{\mathrm{far}}(\boldsymbol{x},\omega),\\
G_{kl}^{\mathrm{near}}(\boldsymbol{x},\omega) &= \frac{3N_kN_l-\delta_{kl}}{4\pi\rho r}\left\{\frac{1}{\alpha^2}\exp\left(\mathrm{i}\omega\frac{r}{\alpha}\right)\left[\left(-\frac{\alpha}{\mathrm{i}\omega r}\right)+\left(-\frac{\alpha}{\mathrm{i}\omega r}\right)^2\right]\right.\\
&\quad\left.-\frac{1}{\beta^2}\exp\left(\mathrm{i}\omega\frac{r}{\beta}\right)\left[\left(-\frac{\beta}{\mathrm{i}\omega r}\right)+\left(-\frac{\beta}{\mathrm{i}\omega r}\right)^2\right]\right\}\quad\text{and}\\
G_{kl}^{\mathrm{far}}(\boldsymbol{x},\omega) &= \frac{1}{4\pi\rho r}\left\{\frac{N_kN_l}{\alpha^2}\exp\left(\mathrm{i}\omega\frac{r}{\alpha}\right)-\frac{N_kN_l-\delta_{kl}}{\beta^2}\exp\left(\mathrm{i}\omega\frac{r}{\beta}\right)\right\},
\end{aligned}
\tag{A 1}
$$

where $G_{kl}^{\mathrm{near}}(\boldsymbol{x},\omega)$ and $G_{kl}^{\mathrm{far}}(\boldsymbol{x},\omega)$ are the near-field and far-field terms of the Green's function, respectively. Vector $\boldsymbol{N}$ is the ray direction; δ_{kl} is the Kronecker delta; ρ is the density of the medium; r is the distance; and $\alpha=\sqrt{a_{11}}$ and $\beta=\sqrt{a_{44}}$ are the velocities of the P and S waves. All quantities in (A 1) are real valued except for the complex-valued velocities α and β.

Appendix B. Green's functions in simple anisotropic viscoelastic media

Here, I mention Green's functions in a closed form for three simple types of anisotropy. The first anisotropy displays an orthorhombic symmetry and the other two types display transverse isotropy. In all cases, the complex-valued slowness surfaces of waves are either ellipsoids, spheroids or spheres. The viscoelastic Green's functions are obtained by expressing the elastic Green's functions in the frequency domain, and by substituting the real-valued elastic parameters by complex-valued viscoelastic parameters. The elastic Green's functions have been published by Payton (1983), Burridge *et al.* (1993) and Vavryčuk (2001).

(*a*) *Anisotropy I*

Let us consider an orthorhombic medium with the following density-normalized viscoelastic coefficients: a_{11}, a_{22}, a_{33}, a_{44}, a_{55}, a_{66}, $a_{12}=-a_{66}$, $a_{13}=-a_{55}$ and $a_{23}=-a_{44}$; the other coefficients being zero. The exact formula for the Green's function reads

$$G_{kl}^{\mathrm{exact}}(\boldsymbol{x},\omega)=\frac{1}{4\pi\rho}\left\{\frac{\delta_{k1}\delta_{l1}}{\sqrt{a_{11}a_{55}a_{66}}}\frac{\exp(\mathrm{i}\omega\tau^{(1)})}{\tau^{(1)}}+\frac{\delta_{k2}\delta_{l2}}{\sqrt{a_{22}a_{44}a_{66}}}\frac{\exp(\mathrm{i}\omega\tau^{(2)})}{\tau^{(2)}}+\frac{\delta_{k3}\delta_{l3}}{\sqrt{a_{33}a_{44}a_{55}}}\frac{\exp(\mathrm{i}\omega\tau^{(3)})}{\tau^{(3)}}\right\}, \tag{B 1}$$

where

$$\tau^{(1)}=r\sqrt{\frac{N_1^2}{a_{11}}+\frac{N_2^2}{a_{66}}+\frac{N_3^2}{a_{55}}},\quad \tau^{(2)}=r\sqrt{\frac{N_1^2}{a_{66}}+\frac{N_2^2}{a_{22}}+\frac{N_3^2}{a_{44}}}\quad\text{and}$$

$$\tau^{(3)}=r\sqrt{\frac{N_1^2}{a_{55}}+\frac{N_2^2}{a_{44}}+\frac{N_3^2}{a_{33}}},$$

are travel times; r is the distance; δ_{kl} is the Kronecker delta; and $\boldsymbol{N}=\boldsymbol{x}/r$ is the ray direction. All quantities in (B 1) are real-valued except for the complex-valued viscoelastic parameters a_{ij} and travel times τ.

Green's function (B 1) is probably the simplest Green's function, which can be found in anisotropic viscoelastic media. It consists of the far-field terms only. No near-field terms and no effects connected to intersection singularities, which are present in the wave field, are observed.

(*b*) *Anisotropy II*

Let us consider a transversely isotropic medium with a vertical axis of symmetry and with the following density-normalized viscoelastic coefficients: a_{11}, $a_{22}=a_{11}$, a_{33}, a_{44}, $a_{55}=a_{44}$, a_{66}, $a_{12}=a_{11}-2a_{66}$, $a_{13}=-a_{44}$ and $a_{23}=-a_{44}$; the

other coefficients being zero. The exact formula for the Green's function reads

$$
\begin{aligned}
G_{kl}^{\mathrm{exact}}(\boldsymbol{x},\omega) &= G_{kl}^{\mathrm{near}}(\boldsymbol{x},\omega) + G_{kl}^{\mathrm{far}}(\boldsymbol{x},\omega),\\
G_{kl}^{\mathrm{near}}(\boldsymbol{x},w) &= \frac{1}{4\pi\rho\sqrt{a_{44}}}\,\frac{g_k^{(2)}g_l^{(2)}-g_k^{(3)}g_l^{(3)}}{R^2}\left(\frac{-1}{\mathrm{i}\omega}\right)\left[\exp(\mathrm{i}\omega\tau^{(3)})-\exp(\mathrm{i}\omega\tau^{(2)})\right],\\
G_{kl}^{\mathrm{far}}(\boldsymbol{x},\omega) &= \frac{1}{4\pi\rho}\left\{\frac{g_k^{(1)}g_l^{(1)}}{a_{44}\sqrt{a_{33}}}\,\frac{\exp(\mathrm{i}\omega\tau^{(1)})}{\tau^{(1)}}+\frac{g_k^{(2)}g_l^{(2)}}{a_{11}\sqrt{a_{44}}}\,\frac{\exp(\mathrm{i}\omega\tau^{(2)})}{\tau^{(2)}}\right.\\
&\quad\left.+\frac{g_k^{(3)}g_l^{(3)}}{a_{66}\sqrt{a_{44}}}\,\frac{\exp(\mathrm{i}\omega\tau^{(3)})}{\tau^{(3)}}\right\},
\end{aligned}
\tag{B 2}
$$

where

$$
\tau^{(1)} = \frac{r}{\sqrt{a_{44}}}\sqrt{N_1^2+N_2^2+\frac{a_{44}}{a_{33}}N_3^2},\quad \tau^{(2)} = \frac{r}{\sqrt{a_{11}}}\sqrt{N_1^2+N_2^2+\frac{a_{11}}{a_{44}}N_3^2},
$$

$$
\tau^{(3)} = \frac{r}{\sqrt{a_{66}}}\sqrt{N_1^2+N_2^2+\frac{a_{66}}{a_{44}}N_3^2}
$$

are travel times,

$$
\boldsymbol{g}^{(1)} = \begin{bmatrix}0\\0\\1\end{bmatrix},\quad \boldsymbol{g}^{(2)} = \frac{1}{\sqrt{N_1^2+N_2^2}}\begin{bmatrix}N_1\\N_2\\0\end{bmatrix},\quad \boldsymbol{g}^{(3)} = \frac{1}{\sqrt{N_1^2+N_2^2}}\begin{bmatrix}N_2\\-N_1\\0\end{bmatrix},
$$

are polarization vectors; r is the distance of the observation point from the source; $R=\sqrt{x_1^2+x_2^2}$ is the distance of the observation point from the symmetry axis; and $\boldsymbol{N}=\boldsymbol{x}/r$ is the ray direction. All quantities in (B 2) are real-valued except for complex-valued viscoelastic parameters a_{ij} and travel times τ.

The Green's function (B 2) consists of the far-field term as well as of the near-singularity term (see Vavryčuk 1999). The near-singularity term is significant near the symmetry axis, where a kiss singularity is observed. The amplitude of this term decreases with distance R from the singularity as $1/R^2$. Physically, the near-singularity term represents the coupling between the SV and SH waves (Vavryčuk 1999, 2006*b*).

(*c*) *Anisotropy III*

Let us consider a transversely isotropic medium with a vertical axis of symmetry and with the following density-normalized viscoelastic coefficients: a_{11}, $a_{22}=a_{11}$, $a_{33}=a_{11}$, a_{44}, $a_{55}=a_{44}$, a_{66}, $a_{12}=a_{11}-2a_{66}$, $a_{13}=a_{11}-2a_{44}$ and $a_{23}=a_{11}-2a_{44}$; the other coefficients being zero. The exact formula for the

Green's function reads

$$
\begin{aligned}
G_{kl}^{\mathrm{exact}}(\boldsymbol{x},\omega) &= G_{kl}^{\mathrm{near}}(\boldsymbol{x},\omega) + G_{kl}^{\mathrm{far}}(\boldsymbol{x},\omega),\\
G_{kl}^{\mathrm{near}}(\boldsymbol{x},\omega) &= \frac{1}{4\pi\rho\sqrt{a_{44}}}\,\frac{g_k^{(3)\perp}g_l^{(3)\perp} - g_k^{(3)}g_l^{(3)}}{R^2}\left(\frac{-1}{\mathrm{i}\omega}\right)\left[\exp(\mathrm{i}\omega\tau^{(3)}) - \exp(\mathrm{i}\omega\tau^{(2)})\right]\\
&\quad + \frac{3g_k^{(1)}g_l^{1} - \delta_{kl}}{4\pi\rho r}\left\{\frac{1}{a_{11}}\exp(\mathrm{i}\omega\tau^{(1)})\left[\left(\frac{-1}{\mathrm{i}\omega\tau^{(1)}}\right) + \left(\frac{-1}{\mathrm{i}\omega\tau^{(1)}}\right)^2\right]\right.\\
&\quad \left. - \frac{1}{a_{44}}\exp(\mathrm{i}\omega\tau^{(2)})\left[\left(\frac{-1}{\mathrm{i}\omega\tau^{(2)}}\right) + \left(\frac{-1}{\mathrm{i}\omega\tau^{(2)}}\right)^2\right]\right\}\\
G_{kl}^{\mathrm{far}}(\boldsymbol{x},\omega) &= \frac{1}{4\pi\rho}\left\{\frac{g_k^{(1)}g_l^{(1)}}{\sqrt{a_{11}^3}}\,\frac{\exp(\mathrm{i}\omega\tau^{(1)})}{\tau^{(1)}} + \frac{g_k^{(2)}g_l^{(2)}}{\sqrt{a_{44}^3}}\,\frac{\exp(\mathrm{i}\omega\tau^{(2)})}{\tau^{(2)}} + \frac{g_k^{(3)}g_l^{(3)}}{a_{66}\sqrt{a_{44}}}\,\frac{\exp(\mathrm{i}\omega\tau^{(3)})}{\tau^{(3)}}\right\},
\end{aligned}
\tag{B 3}
$$

where

$$
\tau^{(1)} = \frac{r}{\sqrt{a_{11}}}, \quad \tau^{(2)} = \frac{r}{\sqrt{a_{44}}}, \quad \tau^{(3)} = \frac{r}{\sqrt{a_{66}}}\sqrt{N_1^2 + N_2^2 + \frac{a_{66}}{a_{44}}N_3^2}
$$

are travel times;

$$
\boldsymbol{g}^{(1)} = \begin{bmatrix} N_1\\ N_2\\ N_3\end{bmatrix}, \quad \boldsymbol{g}^{(2)} = \frac{1}{\sqrt{N_1^2+N_2^2}}\begin{bmatrix} -N_1N_3\\ -N_2N_3\\ N_1^2+N_2^2\end{bmatrix}, \quad \boldsymbol{g}^{(3)} = \frac{1}{\sqrt{N_1^2+N_2^2}}\begin{bmatrix} N_2\\ -N_1\\ 0\end{bmatrix}
$$

are polarization vectors; r is the distance of the observation point from the source; $R = \sqrt{x_1^2 + x_2^2}$ is the distance of the observation point from the symmetry axis; and $\boldsymbol{N} = \boldsymbol{x}/r$ is the ray direction. All quantities in (B 3) are real-valued, except for complex-valued viscoelastic parameters a_{ij} and travel times τ.

The Green's function (B 3) consists of the far-field term as well as the near-field and near-singularity terms. The near-field term represents the coupling between the P and SV waves and is analogous to the near-field term observed in isotropic media (A 1). The near-singularity term is significant near the symmetry axis, similarly as in anisotropy II (B 2).

References

Aki, K. & Richards, P. G. 2002 *Quantitative seismology*. Sausalito, CA: University Science Books.

Auld, B. A. 1973 *Acoustic fields and waves in solids*. New York, NY: Wiley.

Ben-Menahem, A. & Singh, S. J. 1981 *Seismic waves and sources*. New York, NY: Springer.

Borcherdt, R. D. 1977 Reflection–refraction of type-II S waves in elastic and anelastic media. *Bull. Seism. Soc. Am.* **67**, 43–67.

Borcherdt, R. D. 1982 Reflection–refraction of general P- and type-I S waves in elastic and anelastic solids. *Geophys. J. R. Astron. Soc.* **70**, 621–638.

Boulanger, P. 1998 Energy flux for damped inhomogeneous plane waves in viscoelastic fluids. *Wave Motion* **28**, 215–225. (doi:10.1016/S0165-2125(98)00011-0)

Brokešová, J. 2001 Reflection/transmission coefficients at a plane interface in dissipative and nondissipative isotropic media: a comparison. *J. Comput. Acoust.* **9**, 623–641. (doi:10.1142/S0218396X01000760)

Buchwald, V. T. 1959 Elastic waves in anisotropic media. *Proc. R. Soc. A* **253**, 563–580. (doi:10.1098/rspa.1959.0221)

Burridge, R. 1967 The singularity on the plane lids of the wave surface of elastic media with cubic symmetry. *Q. J. Mech. appl. Math.* **20**, 41–56. (doi:10.1093/qjmam/20.1.41)

Burridge, R., Chadwick, P. & Norris, A. N. 1993 Fundamental elastodynamic solutions for anisotropic media with ellipsoidal slowness surfaces. *Proc. R. Soc. A* **440**, 655–681. (doi:10.1098/rspa.1993.0039)

Carcione, J. M. 1990 Wave propagation in anisotropic linear viscoelastic media: theory and simulated wavefields. *Geophys. J. Int.* **101**, 739–750. [Erratum in *Geophys. J. Int.* 1992, **111**, 191.] (doi:10.1111/j.1365-246X.1990.tb05580.x)

Carcione, J. M. 1994 Wavefronts in dissipative anisotropic media. *Geophysics* **59**, 644–657. (doi:10.1190/1.1443624)

Carcione, J. M. 2001 *Wave fields in real media: wave propagation in anisotropic, anelastic and porous media*. Amsterdam, The Netherlands: Pergamon.

Carcione, J. M. & Cavallini, F. 1993 Energy balance and fundamental relations in anisotropic–viscoelastic media. *Wave Motion* **18**, 11–20. (doi:10.1016/0165-2125(93)90057-M)

Carcione, J. M. & Cavallini, F. 1995 Attenuation and quality factor surfaces in anisotropic–viscoelastic media. *Mech. Mater.* **19**, 311–327. (doi:10.1016/0167-6636(94)00040-N)

Caviglia, G. & Morro, A. 1992 *Inhomogeneous waves in solids and fluids*. Singapore: World Scientific.

Červený, V. 2001 *Seismic ray theory*. Cambridge, UK: Cambridge University Press.

Červený, I. & Pšenčík, V. 2005 Plane waves in viscoelastic anisotropic media—I. Theory. *Geophys. J. Int.* **161**, 197–212. (doi:10.1111/j.1365-246X.2005.02589.x)

Červený, V. & Pšenčík, I. 2006 Energy flux in viscoelastic anisotropic media. *Geophys. J. Int.* **166**, 1299–1317. (doi:10.1111/j.1365-246X.2006.03057.x)

Daley, P. F. & Krebes, E. S. 2004 *SH* wave propagation in viscoelastic media. *Stud. Geophys. Geod.* **48**, 563–587. (doi:10.1023/B:SGEG.0000037472.40481.cd)

Deschamps, M., Poirée, B. & Poncelet, O. 1997 Energy velocity of complex harmonic plane waves in viscous fluids. *Wave Motion* **25**, 51–60. (doi:10.1016/S0165-2125(96)00032-7)

Every, A. G. & Kim, K. Y. 1994 Time domain dynamic response functions of elastically anisotropic solids. *J. Acoust. Soc. Am.* **95**, 2505–2516. (doi:10.1121/1.409860)

Gridin, D. 2000 Far-field asymptotics of the Green tensor for a transversely isotropic solid. *Proc. R. Soc. A* **456**, 571–591. (doi:10.1098/rspa.2000.0531)

Hosten, B., Deschamps, M. & Tittmann, B. R. 1987 Inhomogeneous wave propagation in lossy anisotropic solids. Application to the characterization of viscoelastic composite materials. *J. Acoust. Soc. Am.* **82**, 1763–1770. (doi:10.1121/1.395170)

Klimeš, L. 2002 Relation of the wave-propagation metric tensor to the curvatures of the slowness and ray-velocity surfaces. *Stud. Geophys. Geod.* **46**, 589–597. (doi:10.1023/A:1019551320867)

Krebes, E. S. 1983 The viscoelastic reflection/transmission problem: two special cases. *Bull. Seism. Soc. Am.* **73**, 1673–1683.

Moczo, P., Robertsson, J. O. A. & Eisner, L. 2007 The finite-difference time-domain method for modelling of seismic wave propagation. In *Advances in wave propagation in heterogeneous Earth*, vol. 48 (eds R.-S. Wu, V. Maupin & R. Dmowska). Advances in geophysics, pp. 421–516. Amsterdam, The Netherlands: Elsevier/Academic Press.

Mura, T. 1987 *Micromechanics of defects in solids*, 2nd edn. Dordrecht, The Netherlands: Martinus Nijhoff.

Nechtschein, S. & Hron, F. 1996 Reflection and transmission coefficients between two anelastic media using asymptotic ray theory. *Can. J. Expl. Geophys.* **32**, 31–40.

Norris, A. N. 1994 Dynamic Green functions in anisotropic piezoelectric, thermoelastic and poroelastic solids. *Proc. R. Soc. A* **447**, 175–188. (doi:10.1098/rspa.1994.0134)

Payton, R. G. 1983 *Elastic wave propagation in transversely isotropic media*. The Hague, The Netherlands: Martinus Nijhoff Publishers.

Press, W. H., Teukolsky, S. A., Vetterling, W. T. & Flannery, B. P. 2002 *Numerical recipes: the art of scientific computing*. Cambridge, UK: Cambridge University Press.

Richards, P. G. 1984 On wavefronts and interfaces in anelastic media. *Bull. Seism. Soc. Am.* **74**, 2157–2165.

Saenger, E. H. & Bohlen, T. 2004 Finite-difference modeling of viscoelastic and anisotropic wave propagation using the rotated staggered grid. *Geophysics* **69**, 583–591. (doi:10.1190/1.1707078)

Shuvalov, A. L. 2001 On the theory of plane inhomogeneous waves in anisotropic elastic media. *Wave Motion* **34**, 401–429. (doi:10.1016/S0165-2125(01)00080-4)

Shuvalov, A. L. & Scott, N. H. 1999 On the properties of homogeneous viscoelastic waves. *Q. J. Mech. Appl. Math* **52**, 405–417. (doi:10.1093/qjmam/52.3.405)

Vavryčuk, V. 1999 Properties of *S* waves near a kiss singularity: a comparison of exact and ray solutions. *Geophys. J. Int.* **138**, 581–589. (doi:10.1046/j.1365-246X.1999.00887.x)

Vavryčuk, V. 2001 Exact elastodynamic Green functions for simple types of anisotropy derived from higher-order ray theory. *Stud. Geophys. Geod.* **45**, 67–84. (doi:10.1023/A:1021754530968)

Vavryčuk, V. 2002 Asymptotic elastodynamic Green function in the kiss singularity in homogeneous anisotropic solids. *Stud. Geophys. Geod.* **46**, 249–266. (doi:10.1023/A:1019854020095)

Vavryčuk, V. 2003 Parabolic lines and caustics in homogeneous weakly anisotropic solids. *Geophys. J. Int.* **152**, 318–334. (doi:10.1046/j.1365-246X.2003.01845.x)

Vavryčuk, V. 2006*a* Calculation of the slowness vector from the ray vector in anisotropic media. *Proc. R. Soc. A* **462**, 883–896. (doi:10.1098/rspa.2005.1605)

Vavryčuk, V. 2006*b* Comment to "qS-waves in a vicinity of the axis of symmetry of homogeneous transversely isotropic media", by M. Popov, G. F. Passos, and M. A. Botelho [Wave Motion 42 (2005) 191–201]. *Wave Motion* **44**, 128–136. (doi:10.1016/j.wavemoti.2006.08.004)

Wang, C.-Y. & Achenbach, J. D. 1994 Elastodynamic fundamental solutions for anisotropic solids. *Geophys. J. Int.* **118**, 384–392. (doi:10.1111/j.1365-246X.1994.tb03970.x)

Wennerberg, L. 1985 Snell's law for viscoelastic materials. *Geophys. J. Roy. Astron. Soc.* **81**, 13–18.

Willis, J. R. 1980 A polarization approach to the scattering of elastic waves. I. Scattering by a single inclusion. *J. Mech. Phys. Solids* **28**, 287–305. (doi:10.1016/0022-5096(80)90021-6)

Zhu, Y. & Tsvankin, I. 2006 Plane-wave propagation in attenuative transversely isotropic media. *Geophysics* **71**, T17–T30. (doi:10.1190/1.2187792)

Zhu, Y. & Tsvankin, I. 2007 Plane-wave attenuation anisotropy in orthorhombic media. *Geophysics* **72**, D9–D19. (doi:10.1190/1.2387137)